PHYSICAL REVIEW A **80**, 031805(R) (2009)

Phase-reversal diffraction in incoherent light

Su-Heng Zhang,[1] Shu Gan,[1] De-Zhong Cao,[2] Jun Xiong,[1] Xiangdong Zhang,[1] and Kaige Wang[1,*]
[1]*Department of Physics, Applied Optics Beijing Area Major Laboratory, Beijing Normal University, Beijing 100875, China*
[2]*Department of Physics, Yantai University, Yantai 264005, China*
(Received 29 May 2009; published 30 September 2009)

Phase reversal occurs in the propagation of an electromagnetic wave in a negatively refracting medium or a phase-conjugate interface. Here we report the experimental observation of phase-reversal diffraction without the above devices. Our experimental results and theoretical analysis demonstrate that phase-reversal diffraction can be formed through the first-order field correlation of chaotic light. The experimental realization is similar to the phase-reversal behavior in negatively refracting media.

DOI: 10.1103/PhysRevA.80.031805 PACS number(s): 42.30.Rx, 42.87.Bg, 42.30.Wb

Diffraction changes the wave front of a traveling wave. A lens is a key device that can modify the wave front and perform imaging. The complete recovery of the wave front is possible if its phase evolves backward in time in which case an object can be imaged to give an exact copy. A phase-conjugate mirror formed by a four-wave mixing process is able to generate the conjugate wave with respect to an incident wave and thus achieve lensless imaging [1]. A slab of negative refractive-index material can play a role similar to a lens in performing imaging [2–7]. Pendry in a recent paper [8] explored the similarity between a phase-conjugate interface and negative refraction and pointed out their intimate link to time reversal. An experiment to realize a negatively refracting lens by means of phase-conjugate interfaces was also proposed.

Here we report an experiment which demonstrates that phase-reversal diffraction can occur through the first-order spatial correlation of chaotic light using neither negative refraction nor a phase-conjugate interface. The experimental setup is an interferometer as shown in Fig. 1. An object is placed in one arm of the interferometer, while a glass rod with a refractive index $n=1.5163$ is inserted in the other arm. The two ends of the rod are plane. The interferometer is illuminated by an incoherent light source, a Na lamp of wavelength 589.3 nm with an extended illumination area of 10×10 mm^2. Interference patterns of the interferometer can be recorded by either of two charge-coupled device (CCD) cameras. The traveling distances from the source to the detection plane of the CCD cameras through the object and reference arms are $z_o=41.8$ cm and $z_r=33.8$ cm, respectively. When the length of the glass rod is $l=15.5$ cm, the two arms of the interferometer have the same optical path although their physical lengths are different. Under the equal-optical-path condition, the two fields to be interfered in the detection plane come from the same wave front of the source. We will show later that a medium in the path changes its diffraction length away from optical path. The diffraction length of the reference path can be calculated as $\bar{Z}=z_r-l+l/n=28.5$ cm. If phase-reversal diffraction exists, we may predict that the recovery of wave front will occur at a certain place. When the object is placed at a distance $z_{o1}=\bar{Z}$ from the source, we observe its image on the CCD screen, as shown in Fig. 2. The left column in Fig. 2 shows the images of an amplitude-modulated object of two Chinese characters (China), and the right one is for a phase-modulated object which consists of two transparent holes, having a path difference of about a half wavelength. We can see that the two patterns of Figs. 2(a) and 2(b) recorded by the two CCD cameras, respectively, have a phase difference of π. Since BS_2 is a 50/50 beamsplitter, the intensity background can be eliminated through the difference between (a) and (b), and the visibility of the image is enhanced, as shown in Fig. 2(c). On the contrary, the images are erased when we take the sum of (a) and (b), leaving only the intensity background of the two beams, as shown in Fig. 2(d). For an object consisting of the two holes, the images exhibit distinct phase contrast: when one is bright, the other is dark. The imaging scheme is evidently phase sensitive.

We now use a double slit of slit width $b=125$ μm and spacing $d=300$ μm as the object and compare the interference patterns in the same configuration using spatially incoherent and coherent light. The double slit is placed at the same position as above, and its images are observed in the left part of Fig. 3. Then we insert a pinhole in front of the lamp to improve the spatial coherence. Instead of the image of the double slit, we observe its interference fringes, as shown in the right part of Fig. 3, as expected. As a matter of fact, for coherent interferometry, lensless imaging can never occur no matter where the object is placed. Next, for the incoherent light source, we move the double slit away from

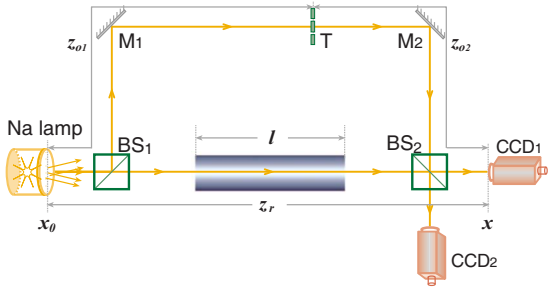

FIG. 1. (Color online) Experimental setup of the interferometer formed by two mirrors M_1 and M_2 and two beamsplitters BS_1 and BS_2. Object T is placed in one arm, while a glass rod is in the other. The interferometer is illuminated by a sodium lamp.

*Corresponding author; wangkg@bnu.edu.cn

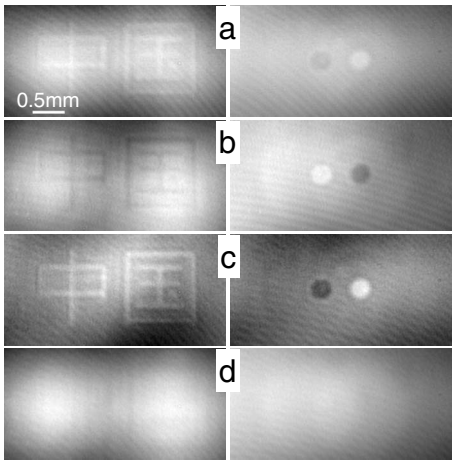

FIG. 2. Experimental results of lensless imaging of two objects placed at the position of $z_{o1}|_{imaging}=28.5$ cm from the source (or $z_{o2}|_{imaging}=13.3$ cm from BS_2). Left column: for an amplitude-modulated object of two Chinese characters (China); right column: for a phase-modulated object of two holes with a phase difference of π. (a) and (b) are the images recorded by the two CCDs; (c) is the difference of (a) and (b) and (d) is their sum, respectively.

the position for imaging. Figures 4(a)–4(e) show the evolution of the interference patterns for $z_{o1}=31.0$, 28.5, 24.2, 20.0, and 10.6 cm, respectively, where Fig. 4(b) corresponds to the image of the double slit.

To understand the experiment, we consider optical diffraction described by $E(x)=\int h(x,x')E_s(x')dx'$, where $E_s(x)$ and $E(x)$ are the field distributions before and after the diffraction, respectively, and $h(x,x')$ is the impulse response function (IRF) of the transverse positions x and x'. In the paraxial propagation, the IRF for free travel over a distance z in homogeneous material is given by [9]

$$H(x,x_0;Z,\bar{Z}) = \sqrt{k_0/(i2\pi\bar{Z})}\exp[ik_0Z + ik_0(x-x_0)^2/(2\bar{Z})], \tag{1}$$

where k_0 is the wave number in vacuum, $Z=nz$ is the optical path and n is the refractive index. We define $\bar{Z}\equiv z/n$ as the diffraction length in the medium.

In a successive diffraction through two media of lengths l_j and indices n_j $(j=1,2)$, we obtain the IRF of the system to be

$$H(x,x_0;n_1l_1+n_2l_2,l_1/n_1+l_2/n_2) = \int H(x,x';n_2l_2,l_2/n_2)H(x',x_0;n_1l_1,l_1/n_1)dx', \tag{2}$$

where the optical path and the diffraction length in the resultant IRF are $n_1l_1+n_2l_2$ and $l_1/n_1+l_2/n_2$, respectively. In general, the IRF for a series of cascaded media is still given by Eq. (1), where the optical path $Z=n_1l_1+n_2l_2+\cdots$ and the diffraction length $\bar{Z}=l_1/n_1+l_2/n_2+\cdots$.

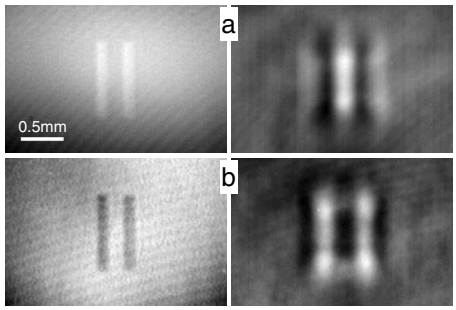

FIG. 3. Experimental results of a double-slit object placed at the same position as that in Fig. 2. Left column: image patterns when the source is spatially incoherent; right column: fringe patterns when the source is spatially coherent (with a pinhole aperture behind the source). Both (a) and (b) were two patterns recorded by the two CCDs.

The diffraction length $\bar{Z}$ can be negative only when a negatively refracting medium is present in the path. The diffraction with a negative diffraction length is phase reversed. In successive diffraction through several media, the phase-reversal diffraction in a negatively refracting medium counteracts the normal one, which may result in $\bar{Z}=0$. In this case, the wave front of the beam is recovered exactly in the propagation, and lensless imaging occurs. Hence, by means of the diffraction theory of light, we have illustrated the imaging condition $\bar{Z}=0$, which is an evidence for the presence of phase-reversal diffraction.

To be specific, we consider the successive diffraction through two media [see Fig. 5(a)]. Let $T(x_0)$ describe a transmittance object, illuminated by a plane wave E_0, then the outgoing field after diffraction is written as

$$E(x) = E_0\int T(x_0)H(x,x_0;n_1l_1+n_2l_2,l_1/n_1+l_2/n_2)dx_0. \tag{3}$$

When $l_1/n_1+l_2/n_2=0$ is fulfilled, Eq. (2) becomes

$$H(x,x_0;n_1l_1+n_2l_2,0) = \exp[ik_0(n_1l_1+n_2l_2)]\times\delta(x-x_0). \tag{4}$$

Hence, we obtain the image $E(x)=E_0\exp[ik_0(n_1l_1+n_2l_2)]T(x)$, and $l_1/n_1+l_2/n_2=0$ signifies the imaging condition. Otherwise, Eq. (3) represents Fresnel

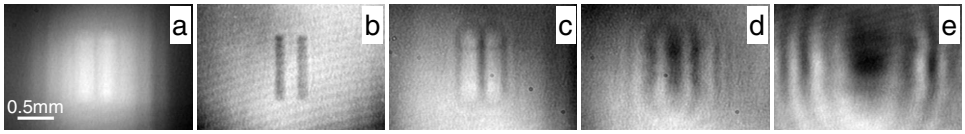

FIG. 4. Diffraction patterns of the double slit. [(a)–(e)] The double slit is placed, respectively, at the positions of $z_{o1}=31.0$, 28.5, 24.2, 20.0, and 10.6 cm, corresponding to the effective diffraction lengths $Z_{eff}=2.0$, 0, −5.7, −13.9, and −42.0 cm. We see that (b) is the image of the double slit.

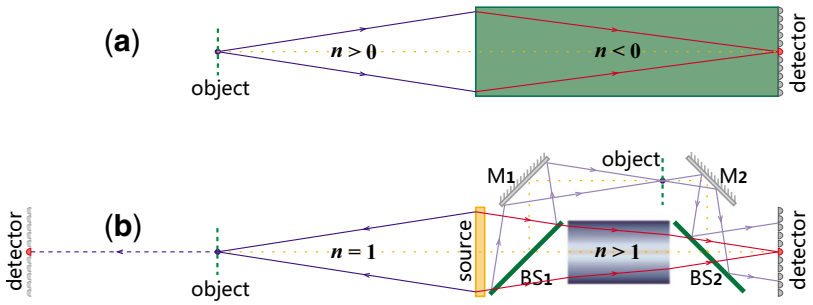

FIG. 5. (Color online) Illustration of lensless imaging by the two schemes: (a) imaging via a successive diffraction through two media, where one is a negative refractive-index medium; (b) imaging using an incoherent light interferometer. When the interferometer is opened out and the two arms are set along a line, the joint diffraction through the two arms is comparable with that in (a).

diffraction with a diffraction length of $l_1/n_1+l_2/n_2$.

We return to our experimental scheme in which the incoherent source field $E_s(x)$ is assumed to be quasimonochromatic and satisfies completely spatial incoherence $\langle E_s^*(x)E_s(x')\rangle = I_s\delta(x-x')$, where I_s is the intensity. Let $E_o(x)$ and $E_r(x)$ be the field distributions of the object and reference waves in the recording plane, respectively, then the intensity pattern in the statistical average is given by $\langle I(x)\rangle = \langle E_o^*(x)E_o(x)\rangle + \langle E_r^*(x)E_r(x)\rangle + [\langle E_r^*(x)E_o(x)\rangle + \text{c.c.}]$. The interference term for the incoherent source is obtained as

$$\langle E_r^*(x)E_o(x)\rangle = I_s \int h_r^*(x,x_0)h_o(x,x_0)dx_0, \tag{5}$$

where $h_o(x,x_0)$ and $h_r(x,x_0)$ are the IRFs for the object and reference arms, respectively. Equation (5) establishes a joint diffraction of two waves, one of which acts as a conjugate wave with the other. As for the coherent light, however, the two fields are separable and there is no joint diffraction between them.

In the interferometer, the IRF for the object arm is written as

$$h_o(x,x_0) = \int H(x,x';z_{o2},z_{o2})T(x')H(x',x_0;z_{o1},z_{o1})dx'. \tag{6}$$

The IRF of the reference arm is described by Eq. (1), i.e., $h_r(x,x_0)=H(x,x_0;Z,\bar{Z})$. In the statistical correlation of Eq. (5), the reference wave acts as a conjugate wave that reverses its phase, $H^*(x,x_0;Z,\bar{Z})=H(x,x_0;-Z,-\bar{Z})$, in forming a joint diffraction pattern with the object wave. As shown in Fig. 5(b), when the interferometer is opened out and the two arms are set along a line, the joint diffraction through the two arms is comparable with the successive diffraction through two media, one of which is negatively refracting material.

To realize interference in the interferometer, the optical path difference between the two arms must be less than the longitudinal coherence length of the source. Hence, we assume the equal-optical-path lengths in the interferometer, i.e., $z_o=Z$. If the distance between the object and the source is equal to the diffraction length in the reference arm, $z_{o1}=\bar{Z}$, Eq. (5) becomes

$$\langle E_r^*(x)E_o(x)\rangle = I_s\sqrt{k_0/(2\pi i z_{o2})}T(x). \tag{7}$$

The object has been exactly reconstructed in the detection plane. Otherwise, Eq. (5) is written as

$$\langle E_r^*(x)E_o(x)\rangle = I_s \int T(x')H(x,x';z_{o1}+z_{o2}-Z,Z_{eff})dx', \tag{8}$$

where Z_{eff} is the effective diffraction length, given by $1/Z_{eff}=1/z_{o2}+1/(z_{o1}-\bar{Z})$. Equation (8) displays the Fresnel diffraction pattern of an object propagating a distance Z_{eff}, which is composed of the two diffraction lengths z_{o2} and $z_{o1}-\bar{Z}$. Both imaging (7) and diffraction (8) can find their counterparts in the negative refraction scheme [see Eq. (3)]. We note that the intensities of the two arms $\langle E_o^*(x)E_o(x)\rangle$ and $\langle E_r^*(x)E_r(x)\rangle$ are homogeneously distributed, contributing a flat background to the interference pattern.

For the scheme of Fig. 1, the optical path of the reference arm is $Z=z_r-l+nl=41.8$ cm, which is identical to that of the object arm, while the corresponding diffraction length $\bar{Z}=z_r-l+l/n=28.5$ cm. The latter determines the object's position for imaging, i.e., $z_{o1}|_{imaging}=\bar{Z}$, or equivalently, $z_{o2}|_{imaging}=Z-\bar{Z}=l(n-1/n)=13.3$ cm. When the refractive index is closer to unity, the object's position for imaging approaches the detection plane.

Under the equal-optical-path condition, the effective diffraction length can be expressed as $Z_{eff}=z_{o2}[1-z_{o2}/z_{o2}|_{imaging}]$. Remarkably, our scheme is capable of performing both normal diffraction and phase-reversal diffraction depending on whether the effective diffraction length is positive or negative, respectively. A positive diffraction length is obtained only when $z_{o2}<z_{o2}|_{imaging}$. Figure 4(a) shows the near-field diffraction pattern for $Z_{eff}=2.0$ cm. When $z_{o2}>z_{o2}|_{imaging}$, the diffraction patterns in Figs. 4(c)–4(e) correspond to the negative effective diffraction lengths $Z_{eff}=-5.7$, -13.9, and -42.0 cm, respectively.

In summary, we have demonstrated that phase-reversal diffraction can exist in an interferometer driven by incoherent light. When the diffraction length in the reference arm is equal to the object distance in the object arm, the wave front of the object is reconstructed in the outgoing plane due to the diffraction reversal between the two arms. In the past few years, the phenomenon of lensless "ghost" imaging with thermal light has attracted much attention [10–13]; ghost imaging is performed through intensity correlation measurements based on the Hanbury-Brown and Twiss effect [14,15]. Since the intensity correlation measurement of thermal light records the modulus of the first-order cross field

correlation at two positions, i.e., $|\langle E_r^*(x_1)E_o(x_2)\rangle|^2$, the origin of "lensless" ghost imaging can be explained by reasoning similar to the above. However, it should be pointed out that our interferometer implements first-order interference, which is a basically different phenomenon. The present scheme can be regarded as incoherent interferometry: the first-order spatial interference in an interferometer illuminated by incoherent light [16]. It thus incorporates main properties of both coherent interference and incoherent spatial field correlations. To realize the incoherent interferometry, two arms of interferometer must undergo different diffraction configurations. A positive refraction medium, inserted in one arm of the interferometer, can replace the lens in the interferometric scheme of Ref. [16], just like a negative refraction medium making a lens [3]. However, our imaging scheme can bypass the problem of aberration that comes with lens imaging. In comparison with similar effects in negative refraction schemes, the evanescent wave cannot be recovered in the interferometer containing only positively refracting materials; hence, the issue of surpassing the diffraction limit is still unattainable in the present scheme. In practical applications with ordinary optical devices, our scheme may provide a convenient experimental platform for exploring phase-reversal diffraction and may be valuable in the application of phase contrast imaging techniques, where coherent sources and lenses are unavailable, such as when x ray and electron beams are used.

The authors thank L. A. Wu for helpful discussions. This work was supported by the National Fundamental Research Program of China (Project No. 2006CB921404) and the National Natural Science Foundation of China (Project No. 10874019).

[1] M. Nieto-Vesperinas and E. Wolf, J. Opt. Soc. Am. A **2**, 1429 (1985).
[2] V. G. Veselago, Sov. Phys. Usp. **10**, 509 (1968).
[3] J. B. Pendry, Phys. Rev. Lett. **85**, 3966 (2000).
[4] D. R. Smith, Science **308**, 502 (2005).
[5] N. Fang, H. Lee, C. Sun, and X. Zhang, Science **308**, 534 (2005).
[6] D. O. S. Melville and R. J. Blaikie, Opt. Express **13**, 2127 (2005).
[7] I. I. Smolyaninov, Y. J. Hung, and C. C. Davis, Science **315**, 1699 (2007).
[8] J. B. Pendry, Science **322**, 71 (2008).
[9] J. W. Goodman, *Introduction to Fourier Optics*, 2nd ed. (McGraw-Hill, New York, 1996), Chap. 4, p. 67.
[10] D. Z. Cao, J. Xiong, and K. G. Wang, Phys. Rev. A **71**, 013801 (2005).
[11] G. Scarcelli, V. Berardi, and Y. Shih, Appl. Phys. Lett. **88**, 061106 (2006).
[12] L. Basano and P. Ottonello, Appl. Phys. Lett. **89**, 091109 (2006).
[13] X. H. Chen, Q. Liu, K. H. Luo, and L. A. Wu, Opt. Lett. **34**, 695 (2009).
[14] R. Hanbury-Brown and R. Q. Twiss, Nature (London) **178**, 1046 (1956).
[15] A. Gatti, E. Brambilla, and L. A. Lugiato, Prog. Opt. **51**, 251 (2008).
[16] S. H. Zhang *et al.*, Phys. Rev. Lett. **102**, 073904 (2009).